NANO LETTERS

2006
Vol. 6, No. 1
11−15

Hybrid Single-Nanowire Photonic Crystal and Microresonator Structures

Carl J. Barrelet,[†] Jiming Bao,[‡] Marko Lončar,[‡] Hong-Gyu Park,[†] Federico Capasso,*[,‡] and Charles M. Lieber*[,†,‡]

Department of Chemistry and Chemical Biology and Division of Engineering and Applied Sciences, Harvard University, Cambridge, Massachusetts 02138

Received November 21, 2005

ABSTRACT

We report a hybrid approach for photonic systems that combines chemically synthesized single nanowire emitters with lithographically defined photonic crystal and racetrack microresonator structures. Finite-difference time-domain calculations were used to design nanowire photonic crystal structures where the photonic band gap overlaps the electronic band gap of the nanowire. Photoluminescence (PL) images of cadmium sulfide (CdS) nanowire photonic crystal structures designed in this way demonstrate localized emission from engineered defects and light suppression in regions of the photonic crystal. PL spectroscopy studies of defect-free nanowire photonic crystal structures further demonstrate the photonic band gap or stop band that spans most of the CdS band edge emission spectrum. In addition, single CdS nanowire-racetrack microresonator structures were fabricated, and PL imaging and spectroscopy measurements show good coupling of the nanowire to the microcavity including efficient feedback and amplified spontaneous emission. These hybrid structures exploit unique strengths of bottom-up and top-down approaches and thereby open new opportunities in nanophotonics from efficient and localized light sources to integrated optical processing.

Semiconductor nanowires[1] are emerging as powerful building blocks for exploring a wide-range of nanophotonic devices, including light-emitting diodes,[2,3] lasers,[4−6] active waveguides,[7] and integrated electrooptic modulators.[7a,8] Nanowire laser, active waveguide, and integrated electrooptic modulator structures exploit the optical cavity and/or waveguide properties of the semiconductor material and, thus, are distinct from transparent subwavelength dielectric waveguides, such as fabricated silicon on insulator structures operating at telecommunications wavelengths and silica nanowires,[9] because absorption and emission occur at the semiconductor nanowire band edge. Further progress with these nanowire structures and their potential use as photonic circuit elements could be limited by poor control of the coupling of light in to and out of the nanowires. For example, CdS nanowires with diameters of 100 nm or less suffer from large losses from the nanowire cavity due to poor reflectivity of the end facets.[10]

Hybrid structures that merge nanowire building blocks with top-down fabricated elements could offer a solution to this fundamental issue of coupling light in to and out of nanowires as well as enabling other opportunities. For instance, photonic crystals and resonant microcavities have been used extensively in photonics to control the coupling of light with optical cavities and to create very high quality factor cavities,[11] although to date there have been no reports combining these elements with active nanowires. Herein, we report the first studies of light−matter interaction between single semiconductor nanowires and lithographically defined cavities. We demonstrate that photonic crystal structures can be used to suppress and control spatially the emission from specific regions of a nanowire, and moreover, we show that nanowires can be coupled to microresonators yielding efficient feedback and amplified spontaneous emission.

Our basic hybrid structure consists of a free-standing CdS nanowire core[12] embedded in a one-dimensional (1D) photonic crystal, where the photonic crystal can be fabricated as a uniform periodic grating or containing specifically designed defects as illustrated schematically in Figure 1A. To embed isolated nanowires within designed 1D photonic crystal structures, we adopted the following approach.[13] A 800 nm layer of perfluorovinyl ether cyclopolymer was deposited on a single-crystal silicon substrate, followed by sequential deposition of a 200 nm poly(methyl methacrylate) (PMMA) layer, CdS nanowires, and a final 200 nm PMMA layer. Electron-beam lithography was then used to define a specific photonic crystal structure in the PMMA layers above and below an isolated nanowire. We note that the nanowire is supported within the photonic crystal structure with periodic PMMA and air regions above and below the center axis of the nanowire. A representative scanning electron microscopy (SEM) image of the periodic region of a hybrid

* Corresponding authors. E-mail: capasso@deas.harvard.edu and cml@cmliris.harvard.edu
[†] Department of Chemistry and Chemical Biology.
[‡] Division of Engineering and Applied Sciences.

10.1021/nl0522983 CCC: $33.50
Published on Web 12/23/2005

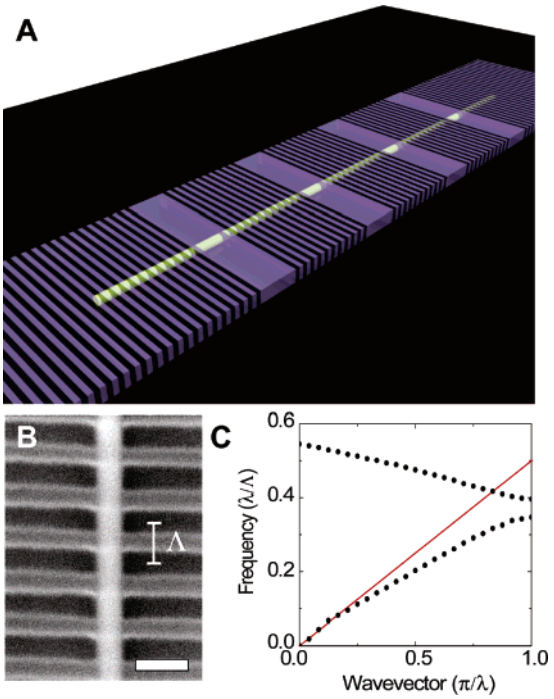

Figure 1. Nanowire photonic crystal structure and modeling. (A) Schematic of the nanowire photonic crystal with four engineered defects. (B) SEM image of a nanowire photonic crystal with a periodicity, $\Lambda = 190$ nm. Scale bar, 200 nm. (C) Dispersion diagram calculated by FDTD simulation showing the presence of a photonic band gap. The red line is the light line in air.

structure is shown in Figure 1B. This image shows that the photonic crystal can be well-aligned relative to the individual, embedded nanowire.

Finite-difference time-domain (FDTD) simulations[14,15] were used to determine the photonic band gap for the hybrid nanowire 1D photonic crystal structures. We evaluated different hybrid structures in order to achieve a good overlap of the photonic band gap with the electronic band gap of the CdS nanowire, 2.5 eV at 300 K.[16] The calculated dispersion diagram for a 90 nm diameter CdS nanowire and 190 nm period 1D photonic crystal (Figure 1C) shows that the photonic crystal behaves as a grating acting strongly on the evanescent field.[15] Specifically, a wide photonic band gap exists in which light propagation along the wire is suppressed. The calculated photonic band gap, $477 < \lambda < 544$ nm, spans the entire emission range of high-quality CdS nanowires, which exhibit an emission peak and full width at half-maximum of 515 and 15 nm, respectively. The position and width of the photonic band gap depend on the nanowire diameter for a given periodicity[17] and thus underscore the importance of the simulations in designing hybrid nanowire/photonic crystal structures that are coupled.

The effect of the photonic band gap on the nanowire photonic crystal hybrid structures was first investigated by introducing one or more PMMA defects in the periodic 1D structure as illustrated schematically in Figure 1A. A typical photoluminescence (PL) image[18] recorded from a CdS nanowire photonic crystal structure with a single defect consisting of the removal of 5 grating periods is shown in Figure 2A. This PL image, which is overlaid with a registered

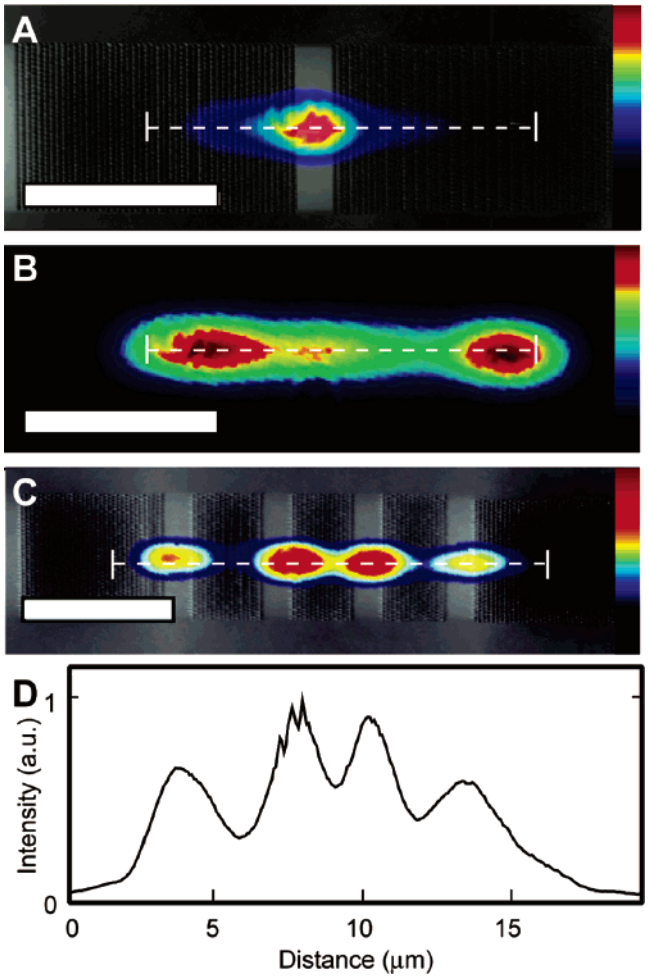

Figure 2. Analysis of nanowire photonic crystal structures containing engineered defects. (A) PL image (false color) superimposed on the AFM image (gray scale) of a nanowire photonic crystal with one defect. Dotted line indicates the nanowire position. Scale bar, 5 μm. (B) PL image of the same nanowire after filling in the photonic crystal structure with PMMA. Scale bar, 5 μm. (C) PL image (false color) superimposed on the AFM image (gray scale) of a nanowire photonic crystal containing four defects, which are visible as vertical lighter gray stripes. Scale bar, 5 μm. (D) Line scan through the PL image in (C) taken along the nanowire axis. The periodicity of the 1D grating regions in (A) and (C) was 180 nm.

atomic-force microscopy (AFM) image of the hybrid structure, demonstrates clearly localized radiation from the artificial defect and inhibition of emission along the nanowire photonic crystal axis, including the nanowire ends. Control experiments involving the deposition of PMMA onto the photonic crystal structures (Figure 2B), which fills in the air gaps and removes the grating, were also carried out to address the effects of electron beam exposure during fabrication. Notably, these PL images show that localized emission is eliminated and conventional nanowire end emission is observed (Figure 2B). Taken together, these data show that the hybrid nanowire photonic crystal structures can spatially control emission from nanowires through the introduction of defects.

To further explore this concept we have fabricated and studied the optical properties of hybrid structures with

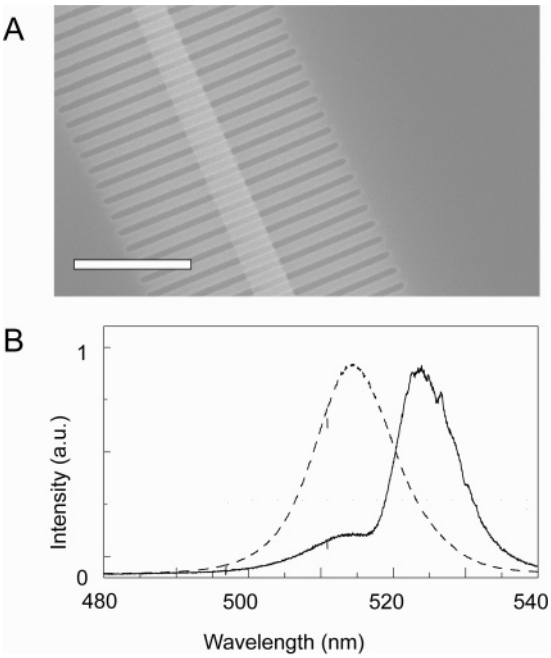

Figure 3. Photonic band gap in a nanowire photonic crystal PL spectrum. (A) SEM image of the hybrid structure consisting of a nanowire with ribbon morphology and surrounding PMMA photonic crystal. Scale bar is 2 μm. The nanowire and orthogonal PMMA grating appear as light gray and the air gaps as thinner dark gray stripes. (B) Normalized photoluminescence spectra with the photonic crystal cladding (solid line) and without (dashed line).

multiple defects introduced in the photonic crystal lattice. For example, a PL image of a structure with four defects is shown in Figure 2C. These data, which are registered to the corresponding AFM image of the hybrid structure, and the line scan in Figure 2D demonstrate localized emission specifically from the four defect sites. In addition, PL spectroscopy studies of the localized emission did not exhibit additional peaks in the CdS emission spectrum. These results suggest either that the cavity mode associated with the defect has a low quality factor or that there is no cavity mode within the emission energy range. While future simulations and experiments will be needed to address further these possibilities, we note that these studies demonstrate for the first time that localized emission is a robust effect in nanowire photonic crystals with engineered defects.

In addition, we have assessed the presence of the predicted photonic band gap in the emission spectrum by fabricating structures to enhance out-of-plane emission from the nanowire. Specifically, a second-order grating will more efficiently scatter light out-of-plane than a first-order grating[14] (used above) and thereby enable better light collection by the objective lens of the PL microscope. A SEM image of one nanowire photonic crystal hybrid structure is shown in Figure 3A. The period of the photonic crystal, $\Lambda = 310$ nm, was optimized using FDTD simulations for overlap of the photonic band gap with the CdS electronic band gap for this larger nanowire.

Significantly, PL spectroscopy of this structure (Figure 3B) shows that the emission is strongly suppressed for most of the CdS band edge spectra, while the PL spectrum recorded from the same nanowire without the photonic crystal shows a typical symmetric spectrum for CdS dominated by band edge emission with peak at 514 nm. The strong contrast between the spectrum with and without the photonic crystal provides direct evidence that the photonic band gap overlaps with the electronic band gap of the nanowire and that photon emission is inhibited due to the presence of the photonic crystal. Previous measurements on CdS nanocluster synthetic opal[19,20] and microsphere[21] hybrids have also shown the presence of photonic band gaps, although our results represent the first direct observation of the photonic band gap in hybrid nanowire structures. In addition, temperature-dependent PL spectroscopy shows that the position of the photonic band gap remains approximately fixed while the nanowire emission shifts with temperature. Together, these studies demonstrate that the photonic band gap in the hybrid nanowire photonic crystal structures can be exploited to tune the nanowire emission spectrum as will be required for many photonics applications.

The generality of our approach for creating hybrid nanowire photonic systems was further explored by fabricating nanowire racetrack microresonator structures. In contrast to 1D photonic crystal cavities based on distributed feedback, nanowire microresonators trap light by total internal reflection, which provides resonant recirculation. An optical micrograph of a representative hybrid structure (Figure 4A) shows the racetrack microresonator defined in PMMA[13] with a 2 μm track width and a 11.2 μm long, 200 nm diameter CdS nanowire embedded in one arm. The total optical length of the resonator, taking into account the refractive indices of PMMA and CdS, is approximately 130 μm.[22]

PL images recorded from the hybrid structure (Figure 4B) show strong emission at the position of the nanowire and also exhibit emission at the edges of the opposite arm of the resonator. These results show that light emitted by the nanowire is guided by total internal reflection around the racetrack microresonator. A representative PL spectrum recorded from the hybrid structure remote to the position of the embedded nanowire is shown in Figure 4C. This spectrum exhibits a progression of relatively sharp, periodic peaks on top of the typical CdS emission that are suggestive of cavity modes. The periodicity of these peaks in terms of inverse wavelengths, 7.9×10^{-3} μm^{-1}, suggests an optical length of ca. 127 μm. An optical length of 126.7 μm was also obtained from the Fourier transform of the PL spectrum plotted versus reciprocal wavelength (inset, Figure 3C). Notably, the optical length determined from the spectra is in excellent agreement with the measured length of the racetrack resonator, 129 μm, and contrasts the 11.2 μm long CdS nanowire cavity length. The optical length can thus be assigned to the fundamental mode circulating around the racetrack microresonator.

Last, we have further probed the nanowire racetrack microresonator hybrid structures by measuring the input/output power dependence at low temperatures. The PL spectrum recorded at 4 K (Figure 4D) exhibits a pronounced peak centered at 485 nm and several satellite peaks corresponding to cavity modes. Significantly, excitation power

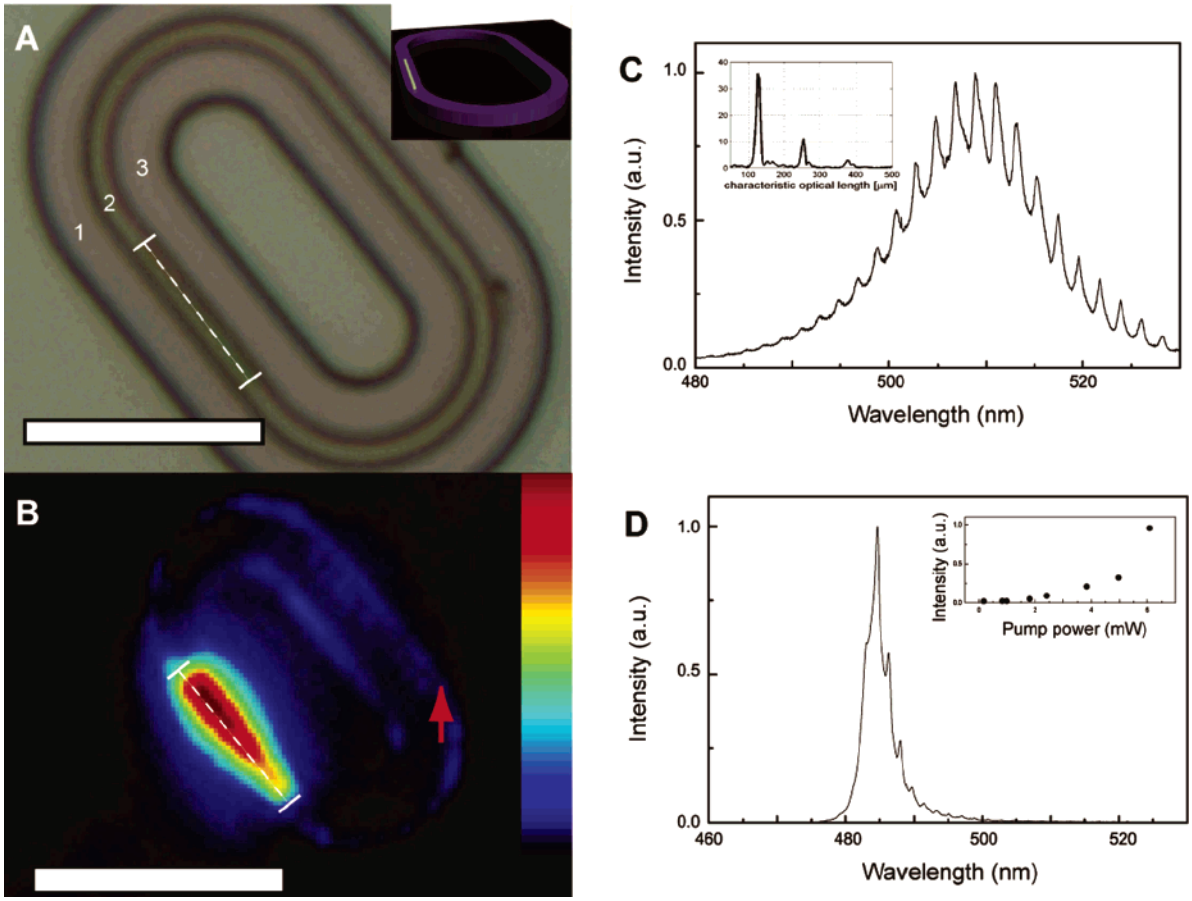

Figure 4. Nanowire racetrack microresonator. (A) White-light optical image of the nanowire/microresonator structure, where regions 1 and 3 correspond to the air surrounding the PMMA racetrack, region 2. The dashed line indicates the nanowire position. Inset, 3D model of the nanowire racetrack microresonator. (B) PL image of the nanowire microresonator. The red arrow indicates the region over which spectra were collected and the dashed line corresponds to position of nanowire as in (A). Both scale bars, 20 μm. (C) PL spectrum recorded at room temperature at location indicated in (B). Inset, Fourier transform of the PL spectrum. (D) PL spectrum at ca. 4 K. Inset, peak output power versus incident pump power.

dependent measurements (inset, Figure 4D) show a superlinear increase in the output emission intensity as a function of incident laser power with an exponent of 2.9. The superlinear increase in the emission output power and the emergence of a dominant mode from the relatively broad spectrum are consistent with amplified stimulated emission from the hybrid structure. We believe that further refinement of the nanowire/microresonator hybrid structures (e.g., reducing the optical losses of the racetrack resonator) has the potential to generate low-threshold external cavity nanowire lasers with the fabricated racetrack enabling a number options beyond that possible with the nanowire alone.

In summary, we have described a hybrid approach for photonic systems that combines bottom-up synthesis of single nanowire emitters with lithographically defined photonic structures. We used this approach to study light−matter interactions at the single nanowire level in two systems, the nanowire 1D photonic crystal and the nanowire racetrack resonator. FDTD calculations were used to design nanowire photonic crystal structures where the photonic band gap overlaps the electronic band gap of the nanowire. PL images of CdS nanowire photonic crystal structures designed in this way demonstrated localized emission from engineered defects and light suppression in regions of the photonic crystal. PL spectroscopy studies of defect-free nanowire photonic crystal structures further showed that the photonic band gap can span most of the CdS band edge emission spectrum and thereby control the nanowire emission spectrum as will be required for many photonics applications. In addition, single CdS nanowire racetrack microresonator structures were fabricated, and PL imaging and spectroscopy measurements showed good coupling of the nanowire to the microcavity including efficient feedback and amplified spontaneous emission. While these studies, which exploit unique strengths of bottom-up and top-down approaches, have focused on single nanowire devices, emerging methods for hierarchical assembly using holographic optical tweezers[23] and other techniques[2a,24] could enable parallel and scalable organization of compact photonic integrated circuits.

Acknowledgment. We thank Chen Yang and Hao Yan for the AFM measurements. H.G.P. acknowledges support from the Korea Research Foundation Grant (KRF-2005-214-C00054). C.M.L. acknowledges support of this work by the Air Force Office of Scientific Research. F.C. acknowledges partial support by the National Science Foundation Nanoscale Science and Engineering Center and by the Center for Nanoscale Science at Harvard University.

References

(1) (a) Hu, J.; Odom, T.; Lieber, C. M. *Acc. Chem. Res.* **1999**, *32*, 435. (b) Lieber, C. M. *MRS Bull.* **2003**, *28*, 486. (c) Yang, P. *MRS Bull.* **2005**, *30*, 85.

(2) (a) Duan, X.; Huang, Y.; Cui, Y.; Wang, J.; Lieber, C. M. *Nature* **2001**, *409*, 66. (b) Zhong, Z.; Qian, F.; Wang, D.; Lieber, C. M. *Nano Lett.* **2003**, *3*, 343. (c) Huang, Y.; Duan, X.; Lieber, C. M. *Small* **2005**, *1*, 142.

(3) (a) Qian, F.; Li, Y.; Gradeèak, S.; Barrelet, C. J.; Wang, D.; Lieber, C. M. *Nano Lett.* **2004**, *4*, 1975. (b) Kim, H.; Cho, Y.; Lee, H.; Kim, S.; Ryu, S. R.; Kim, D. Y.; Kang, T. W.; Chung, K. S. *Nano Lett.* **2004**, *4*, 1059. (c) Qian, F.; Gradecak, S.; Li, Y.; Wen, C.-Y.; Lieber, C. M. *Nano Lett.* **2005**, *5*, 2287.

(4) (a) Huang, M. H.; Mao, S.; Feick, H.; Yan, H.; Wu, Y.; Kind, H.; Weber, E.; Russo, R.; Yang, P. *Science* **2001**, *292*, 1897. (b) Johnson, J. C.; Choi, H. J.; Knutsen, K. P.; Schaller, R. D.; Yang, P.; Saykally, R. J. *Nat. Mater.* **2002**, *1*, 106.

(5) Duan, X.; Huang, Y.; Agarwal, R.; Lieber, C. M. *Nature* **2003**, *421*, 241.

(6) (a) Agarwal, R.; Barrelet, C. J.; Lieber, C. M. *Nano Lett.* **2005**, *5*, 917. (b) Gradecak, S.; Qian, F.; Li, Y.; Park, H.-G.; Lieber, C. M. *Appl. Phys. Lett.* **2005**, *87*, 173111.

(7) (a) Barrelet, C. J.; Greytak, A. B.; Lieber, C. M. *Nano Lett.* **2004**, *4*, 1981. (b) Law, M.; Sirbuly, D. J.; Johnson, J. C.; Goldberger, J.; Saykally, R. J.; Yang, P. *Science* **2004**, *305*, 1269.

(8) Greytak, A. B.; Barrelet, C. J.; Li, Y.; Lieber, C. M. *Appl. Phys. Lett.* **2005**, *87*, 151103.

(9) (a) Vlasov, Y. A.; McNab S. J. *Opt. Express* **2004**, *12*, 1622. (b) Tong, L.; Gattass, R.; Ashcom, J.; He, S.; Lou, J.; Shen, M.; Maxwell, I.; Mazur, E. *Nature* **2003**, *426*, 816.

(10) Maslov, A. V.; Ning, C. Z. *Appl. Phys. Lett.* **2003**, *83*, 1237.

(11) (a) Vahala, K. J. *Nature* **2003**, 424, 839. (b) Joannopolulos, J. D.; Meade, R. D.; Winn, J. N. *Photonic Crystals*; Princeton University Press: Princeton, NJ, 1995.

(12) Barrelet, C. J.; Wu, Y.; Bell, D. C.; Lieber, C. M. *J. Am. Chem. Soc.* **2003**, *125*, 11498.

(13) A 800 nm layer of perfluorovinyl ether cyclopolymer CYTOP/CTL-809M (Asahi Glass, Tokyo Japan) with a refractive index of 1.3 was deposited on a single-crystal silicon substrate, followed by sequential deposition of a 200 nm poly(methyl methacrylate) (PMMA) layer, CdS nanowires, and a final 200 nm PMMA layer. Electron-beam lithography (electron energy = 30 keV) followed by development for 90 s in a solution of methyl isobutyl ketone/isopropyl alcohol, 3:1, was then used to define a specific photonic crystal structure in the PMMA layers above and below an isolated nanowire. A similar procedure was used to define nanowire racetrack microresonantor hybrid structures.

(14) Taflove, A.; Hagness, S. C. *Computational Electrodynamics*; Artech House: Boston, 2000.

(15) The time-dependent Maxwell's equations were solved using the FDTD method on a computational grid with Bloch boundary conditions.[14] This time-domain method is used extensively in the photonic crystal literature to model subwavelength waveguides.[11b] The three inputs in the simulation are (i) a computational unit cell, (ii) an initial field defined as a Dirac pulse in time, with Gausian profile in space, and (iii) a k value. The 3D unit cell consists of one periodicity of the nanowire photonic crystal and is divided into a grid where each point is given a refractive index to best map the hybrid structure; indices of 1, 1.5, and 2.8 were used for air, PMMA, and CdS, respectively. In our simulations, the initial field is located in the nanowire. The FDTD simulation then stores the time evolution of the field. The simulation results were Fourier transformed to convert the field components to the frequency domain, and the field amplitude versus frequency were plotted to determine resonance modes and their corresponding energies. The procedure was repeated for different k values until the dispersion diagram is obtained over the region of interest. The resonance modes depend on both nanowire diameter and photonic crystal periodicity. For small nanowire diameter, the evanescent field is large and consequently the overlap between the field and the photonic crystal is large. For large nanowire diameter, the evanescent field is smaller and correspondingly the overlap between the field and the photonic crystal is small. FDTD calculations provide key guidelines for the design of hybrid structures and interpretation of experiments but could be improved in the future by taking into account absorption and emission processes in the nanowire.

(16) Cardona, M.; Yu, P. Y. *Fundamentals of Semiconductors*; Springer: New York, 2001.

(17) For example, FDTD calculations made on structures with 70 and 126 nm diameter nanowires, which are smaller and larger than actual nanowire, yield calculated photonic band gaps of $430 < \lambda < 510$ nm and $570 < \lambda < 590$ nm, respectively, for a grating periodicity of $\Lambda = 180$ nm.

(18) All nanowire structures studied were optically pumped by a doubled Ti/sapphire laser with a wavelength of 400 nm. The Gaussian laser spot was centered on the nanowire structure, and the spot size was intentionally made large enough to illuminate the entire length of the nanowire. The light emitted from the structure is collected by either a 40× or a 100× objective focused onto the entrance of a 300 mm spectrometer and either imaged or dispersed onto a cooled CCD.

(19) Romanov, S. G.; Fokin, A. V.; Alperovich, V. I,; Johnson, N. P.; De La Rue, R. M. *Phys. Status Solidi A* **1997**, *164*, 169.

(20) Blanco, A.; Lopez C.; Mayoral, R.; Miguez, H.; Meseguer F.; Mifsud A.; Herrero, J. *Appl. Phys. Lett.* **1998**, *73*, 1781.

(21) Lin, Y.; Zhang, J.; Sargent, E. H.; Kumacheva, E. *Appl. Phys. Lett.* **2002**, *81*, 3134.

(22) The path length, L, and the refractive indices, n, are used to estimate the optical length of the racetrack resonator. The length of the PMMA in the racetrack is 64.8 μm and the length of the CdS nanowire is 11.2 μm. The index of PMMA and CdS are 1.5 and 2.8, respectively. $L(\text{PMMA}) \times n(\text{PMMA}) + L(\text{CdS}) \times n(\text{CdS})$ gives a total path length of 129 μm.

(23) Agarwal, R.; Ladavac, K.; Roichman, Y.; Yu, G.; Lieber, C. M.; Grier, D. G. *Opt. Express* **2005**, *13*, 8906.

(24) (a) Huang, Y.; Duan, X.; Wei, Q.; Lieber, C. M. *Science* **2001**, *291*, 630. (b) Whang, D.; Jin, S.; Wu, Y.; Lieber, C. M. *Nano Lett.* **2003**, *3*, 1255.

NL0522983